Science AAAS

Polar Lightning and Decadal-Scale Cloud Variability on Jupiter

Kevin H. Baines, *et al.*

Science **318**, 226 (2007);
DOI: 10.1126/science.1147912

REPORT

Polar Lightning and Decadal-Scale Cloud Variability on Jupiter

Kevin H. Baines,[1] Amy A. Simon-Miller,[2] Glenn S. Orton,[1] Harold A. Weaver,[3] Allen Lunsford,[2] Thomas W. Momary,[1] John Spencer,[4] Andrew F. Cheng,[3] Dennis C. Reuter,[2] Donald E. Jennings,[2] G. R. Gladstone,[5] Jeffrey Moore,[6] S. Alan Stern,[7] Leslie A. Young,[4] Henry Throop,[4] Padma Yanamandra-Fisher,[1] Brendan M. Fisher,[1] Joseph Hora,[8] Michael E. Ressler[1]

Although lightning has been seen on other planets, including Jupiter, polar lightning has been known only on Earth. Optical observations from the New Horizons spacecraft have identified lightning at high latitudes above Jupiter up to 80°N and 74°S. Lightning rates and optical powers were similar at each pole, and the mean optical flux is comparable to that at nonpolar latitudes, which is consistent with the notion that internal heat is the main driver of convection. Both near-infrared and ground-based 5-micrometer thermal imagery reveal that cloud cover has thinned substantially since the 2000 Cassini flyby, particularly in the turbulent wake of the Great Red Spot and in the southern half of the equatorial region, demonstrating that vertical dynamical processes are time-varying on seasonal scales at mid- and low latitudes on Jupiter.

Although lightning has been well documented on the gas giants Jupiter and Saturn at middle and low latitudes (*1*–*13*), it has never been observed in the polar regions. Here we report images of jovian lightning in both hemispheres poleward of 60° latitude obtained with the broadband (0.35- to 0.85-μm bandpass) New Horizons LORRI (Long Range Reconnaissance Imager) camera (*14*). On 3 March 2007, 16 observations were made of the planet's nightside, eight each of the north and south polar regions, consisting of 40 s of total exposure time for each pole. Thirteen lightning strike events were observed poleward of 60° (planetographic) latitude: six in the north polar region and seven in the south polar region (Table 1). The most poleward strikes were at 80°N and 74°S; three separate flashes observed were within 0.5° of 80°N.

Five other lightning strikes were seen near 52°N in 15 s of total exposure time during the three most equatorward observations, which covered latitudes southward to 45°N. Earlier spacecraft (*1*–*7*) had found that the most active lightning region was at latitudes near 50°N. Multiple strikes were seen during a 10-s period within a localized region covering less than 0.7° of longitude in a field of view greater than 35° of longitude. Here, one flash event in a 5-s exposure was followed immediately by at least three spatially separated events in the next 5-s interval (Fig. 1, top row). This corresponds to an average flash rate of 0.4/s (or greater) over 10 s and 0.6/s (or greater) over the single high-activity observation. These rates are greater than the 0.2/s rate previously observed during 60-s scanning exposures by Galileo (*6*, *8*).

Polar lightning flashes integrated over our 5-s exposure times are comparable in brightness to aurorae or the Io Flux Tube in the north polar region (Fig. 1) (*15*). Lightning flashes extend spatially over many pixels in our images (representative lightning flashes are seen in the lower row of images in Fig. 1); each pixel subtends about 28 km at the subspacecraft point on Jupiter (corresponding to 56 km latitudinally at 60°N latitude on the central meridian). This extent indicates that lightning emissions propogated through overlying scattering aerosols or that multiple flashes extended over a large area (typically >10,000 km^2) during the exposure.

The average optical energies per strike in the north and south polar regions were nearly identical, 2.90×10^9 and 2.87×10^9 J for the north and south polar regions, respectively (Table 1) (*16*), despite the large (factor of 5) variability of lightning strength. These values agree well with the mean optical energy of strikes found in nonpolar storms: $2.5 \pm 1.9 \times 10^9$ J (*3*). The largest bolts observed were 9.3×10^9 J in the north and 15.7×10^9 J in the south, which is also in agreement with the largest flashes observed in nonpolar storms by Galileo (*6*). These largest

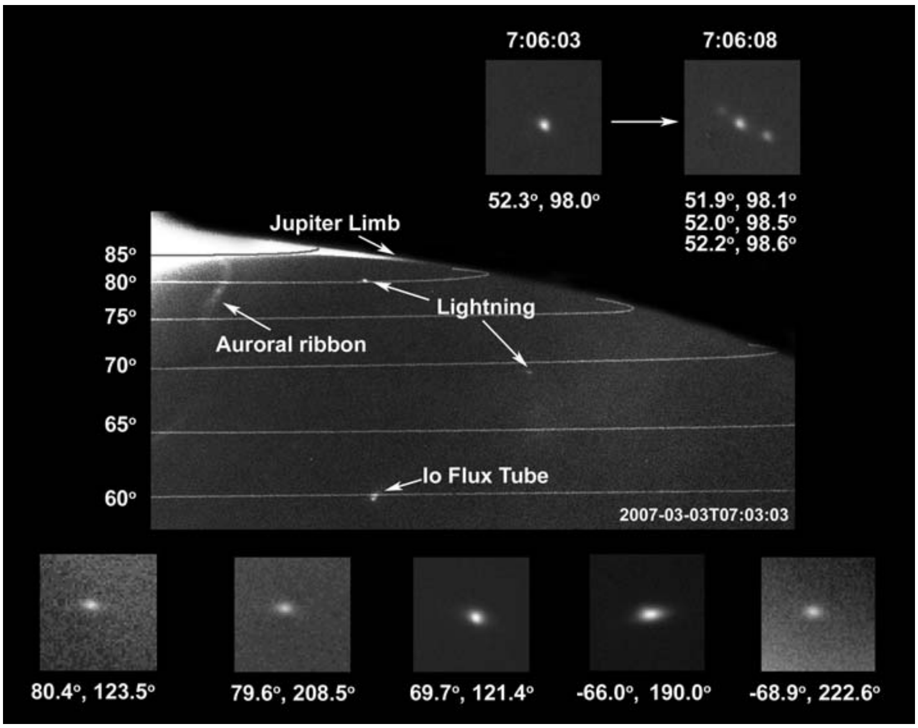

Fig. 1. Representative lightning flashes imaged by LORRI (*14*). (**Top row**) Multiple flashes are observed in consecutive 5-s exposures near 52°N. latitude (planetographic). (**Middle**) Two north polar flashes observed simultaneously in a single 5-s exposure. (**Bottom row**) Flashes in both the north and south polar regions show substantial spatial extension, which is indicative of diffusive aerosol scattering of upwelling emission from near the 5-bar water condensation level.

[1]Jet Propulsion Laboratory, California Institute of Technology, 4800 Oak Grove Drive, Pasadena CA 91109, USA. [2]NASA/Goddard Space Flight Center, Code 693, Greenbelt, MD 20771, USA. [3]The Johns Hopkins University Applied Physics Laboratory, 1110 Johns Hopkins Road, Laurel, MD 20723, USA. [4]Southwest Research Institute, 1050 Walnut Street, Suite 300, Boulder, CO 80302, USA. [5]Southwest Research Institute, 6220 Culebra Road, San Antonio, TX 78238. USA. [6]NASA/Ames Research Center, MS 245-3, Moffett Field, CA 94035–1000, USA. [7]NASA Science Mission Directorate, NASA Headquarters, Washington, DC 20546, USA. [8]Harvard-Smithsonian Center for Astrophysics, 60 Garden Street, Cambridge, MA 02138, USA.

bolts, located near 66° latitude in both hemispheres, were four to five times the mean size and >18 times the smallest strike energies observed in the respective polar regions.

The half-width half-maximum (HWHM) of a lightning flash (the distance over which the lightning radiance falls to half of its peak value) is a measure of the depth of the flash. The New Horizons values (a mean of 92 km) are comparable to those seen in previous investigations (*6*, *8*, *17*) in which flash depths were near the 5- to 8-bar level of water condensation (*18*). Thus, the source of the lightning in our observations was probably also within the deep water-rich regions of Jupiter.

Previous observations found lightning predominantly near 14°N and 50°N (planetographic) and less often at 33°N and 60°N. These appear to mark the southern edges of westward-moving jets (*2*, *4*, *6*) and are regions with notable cyclonic shear. Similarly, the three lightning strikes we saw at the highest latitudes (69° to 71°N, planetographic) coincided with the southern edge of the most northerly westward jet near 72°N discovered by Cassini (*19*).

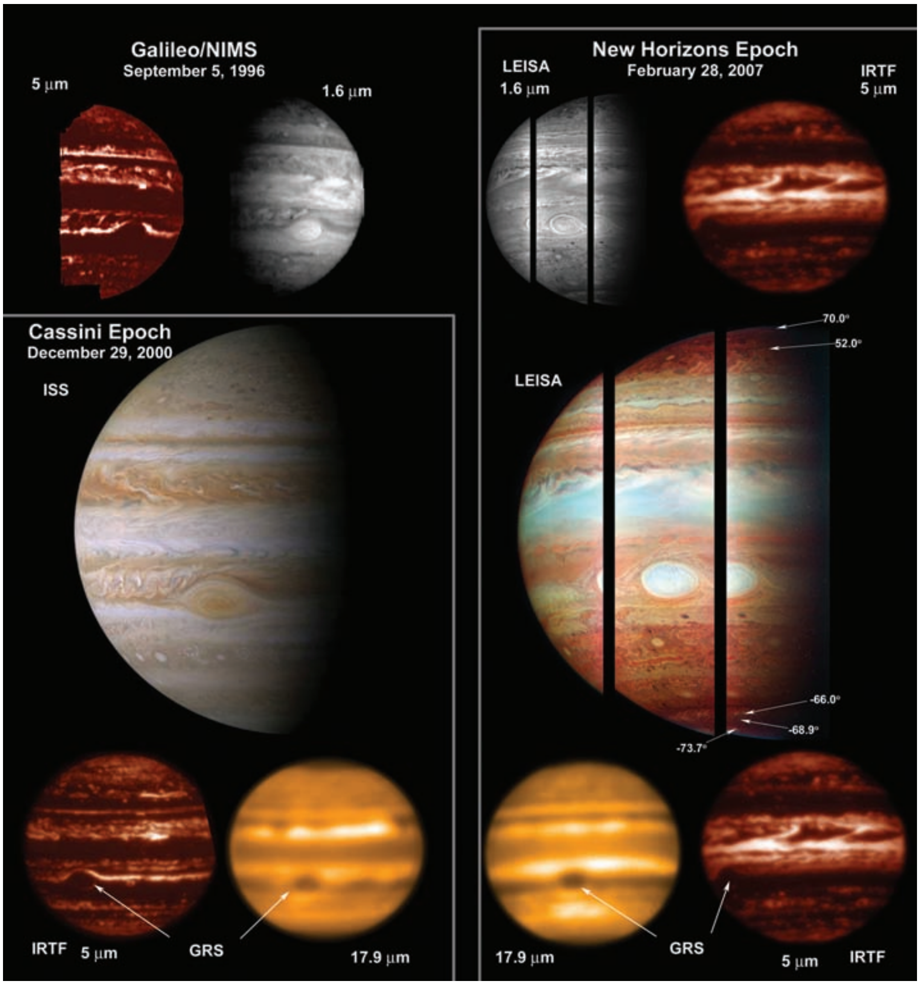

Fig. 2. Global changes in Jupiter's structure: September 1996 (top left) and December 2000 (lower left) versus February 2007 (right). (**Top row**) Near-infrared views of Jupiter from Galileo NIMS in 1996 at 5 µm (red image) and 1.6 µm (gray image) are compared to similar 2007 New Horizons images. Substantial differences in cloud cover are seen in the south equatorial region and northwest of the Great Red Spot (GRS). Similar differences are seen in comparing the 2000 Cassini view (lower left) with the 2007 New Horizons view (right). Here, three global views are shown: three-color images in reflected sunlight (large images), 5-µm thermal imagery (red images, bottom row), and 17.9-µm thermal imagery (orange images, bottom row). The near-natural–color Cassini image is compared to a New Horizons image composed of 1.59-µm (red), 1.90-µm (green), and 1.85-µm (blue) images, emphasizing cloud altitudes and cloud opacities (*28*). The near-uniform thick equatorial cloud structure in 2000 is more complex in 2007, with distinct latitudinal variability in cloud opacity. The increased brightness of the 2007 5-µm images (red images, bottom row) confirms cloud thinning. Little change is seen in the 19.7-µm images (orange), which map 200-mbar-level temperatures. Arrows with labels show several latitudes where polar lightning has been discovered.

These locations are characterized by vigorous upper-level convective clouds and potentially large instabilities (*6*, *20*, *21*). Lightning generally appears near the 5- to 6-bar level (*6*, *8*, *17*), where upwelling water can condense, triggering strong convection and thunderstorms (*2*, *5*, *6*). Vertical transport may be aided by three-dimensional planetary waves, such as have been observed near the equator (*22*, *23*), and by colliding air masses as in the turbulent region to the northwest of the Great Red Spot. Both mechanisms have been observed to produce rapid formation of optically thick ammonia condensation clouds (*23*) and in the latter case, lightning at depth (*24*).

In the southern polar region, only half of the lightning strikes occurred in the cyclonic shear or maximum westward-moving jet regions. In particular, the strikes at 60.2°S and 66°S were on the anticyclonic sides of the two most southerly eastward jets observed by Cassini (*19*). The most polar strikes near 80°N and 74°S were located in regions of weak winds (<10 m/s) and thus also may not be consistent with the westward wind paradigm. The remaining strikes at 68.4°S, 68.9°S, and 71.2°S are consistent with it.

The distribution and power of jovian lightning are different from those on Earth (*5*, *6*). Rather than being concentrated within tens of degrees of the equator, on Jupiter lightning is most optically active near 50°N as observed by every investigating spacecraft (*1*–*7*), now including New Horizons. The distribution of Jovian lightning to high latitudes is probably a consequence of the relative strength of internal heat as compared to solar heating over latitude (*2*, *5*): As one proceeds poleward, solar heating of the atmosphere decreases, allowing the internal heat of Jupiter to power strong vertical dynamics near the 5-bar condensation level of water (*25*, *26*).

Before the New Horizons observations, more and stronger flashes were seen in the northern hemisphere than in the southern at nonpolar latitudes (*5*, *6*). Voyager 2 saw no southern lightning, despite an intense observational campaign (*5*). Such hemispherical differences may be a consequence of slight differences in solar insolation or atmospheric stability. In contrast, New Horizons observed nearly identical rates of lightning strikes in the polar regions (0.15 strikes/s in the north versus 0.18 strikes/s in the south). In each case, about one-fifth of the polar region was viewed at any one time. The mean optical flash energies of the individual northern and southern lightning strikes agree to within 2%. If these average values are representative of all longitudes, the average lightning power per area was about 0.6×10^{-6} and 0.5×10^{-6} W m^{-2} poleward of 60° latitude for the south and north polar regions, respectively. These values are comparable to the optical power measured previously for the nonpolar regions: 0.3 10^{-6} W m^{-2} (*6*) and 0.32 10^{-6} W m^{-2} (*3*).

Thus, over our small sampling of time and longitude, the lightning frequency and optical power in the south and north polar regions agree to within 20%. This similarity suggests that mechanisms that lead to large mid-latitude differences in lightning activity are not important in the polar regions. This view is supported by the Galileo observation (*6*) that, averaged over 5° latitude bins, the greatest number of storms per unit area is observed in the southern hemisphere near 55° latitude (planetographic), but for the broader 45° to 60° latitude region, the northern and southern hemisphere values are comparable. Together, the New Horizons and Galileo high-latitude observations give additional support to the notion that internal heat drives convection and dynamics more effectively in sunlit-poor polar and high-latitude regions than in sunlit-rich equatorial latitudes.

Additional insight into the nature of convection and vertical dynamics on Jupiter is provided by New Horizons global images. These show that vertical dynamics is variable on decadal scales at low and middle latitudes when compared to similar imagery obtained in September 1996 by the Galileo Orbiter and in December 2000 by Cassini-Huygens. The Linear Etalon Infrared Spectral Imager (LEISA) (*27*) on New Horizons obtained a high–spatial-resolution near-infrared global-scale map of Jupiter, timed to provide nearly the same observational and lighting geometry of the Great Red Spot as in the best Galileo near-infrared and Cassini visual imagery (Fig. 2) (*28*).

Distinct differences in cloud cover are seen when directly comparing 1.6-μm images obtained by the Near-Infrared Mapping Spectrometer (NIMS) on Galileo in 1996 (*23*) and the 2007 New Horizons images. This pseudo-continuum wavelength accentuates views of tropospheric clouds found near the 0.5- to 2-bar level. In the 2007 image, these clouds are notably scarcer than in the 1996 image in both the south equatorial region and in the "turbulent wake" region northwest of the Great Red Spot. In 5-μm thermal imagery, the 2007 ground-based images show increased flux, similarly due to the thinning of tropospheric clouds, which allows Jupiter's 5-μm thermal emissions, generated at depth near the 8-bar level, to readily escape out of the atmosphere.

Similar differences in cloud cover are seen between the 2000 Cassini images and the 2007 New Horizons images. The equatorial region is uniformally cloudy in the 2000 Cassini three-color image, whereas the three-color Cassini image shows few clouds in the southern half of this region. Again, the turbulent wake region to the northwest and west of the Great Red Spot is remarkably quiescent in the 2007 image, in stark contrast to the turbulent region of swirling clouds seen in the 2000 image by Cassini and observed consistently for more than 20 years by Voyager, Galileo, and Cassini-Huygens (*1*, *19*, *23*, *29*). This region has been observed to produce the largest spectroscopically identifiable ammonia clouds on Jupiter (*23*), indicative of powerful vertical transport delivering relatively large quantities of ammonia gas to the upper atmosphere. There, large-particle thick clouds are produced on a time scale of a day or less. Yet the 2007 LEISA images show this area almost clear of clouds. Spectroscopic searches for ammonia in this region, such as were successfully conducted with the Galileo NIMS instrument (*23*), show no spectroscopic evidence of ammonia clouds, although such clouds were seen in other regions by LEISA (*30*). The latitudinal region to the west was also clear of thick convective clouds, out to the western limb.

The 5-μm ground-based observations of Jupiter, taken contemporaneously with the Cassini and New Horizons images (Fig. 2, bottom row), confirm the changes in cloud cover. In contrast, the 17.9-μm images of Jupiter, which are indicative of temperatures near the 200-mbar level just below the tropopause, shows few changes between 2000 and 2007.

Thus, the changes seen in 2007 are indicative of changes restricted to tropospheric depths underneath the 200-mbar level. The observed regional changes in mid- and low-latitude cloud properties suggest changes in vertical dynamics and transport, including convection, between ~400 mbar and perhaps several bars. The cause of such changes in vertical dynamics is unclear, but they may be due to variations in atmospheric stability at depth, perhaps due to variations in water content and/or the emission of internal heat. Because the primary driver of Jupiter's global circulation at depth is Jupiter's own internal heat, we suspect that the atypically quiescent view of Jupiter observed by New Horizons and ground-based observations in early 2007 will be relatively short-lived as the planet reverts to its typically dynamic state.

Table 1. Record of lightning strikes observed by New Horizons.

Planetographic latitude	W. longitude (system III)	Image SOC root name	Time on 3 March 2007 (UTC)	Energy (10^9 J)	HWHM of flash (pixels)	HWHM of flash (km)
80.4°N	123.5	lor_0035211303_0x630_sci_1	07:03:02.886	1.46	1.84	81.0
80.1°N	132.5	lor_0035211308_0x630_sci_1	07:03:07.886	0.79	2.75	121.1
79.6°N	208.5	lor_0035219108_0x630_sci_1	09:13:07.886	2.67	2.17	95.6
70.3°N	89.0	lor_0035211663_0x630_sci_1	07:09:02.886	2.64	1.89	83.3
70.1°N	118.3	lor_0035211303_0x630_sci_1	07:03:02.886	0.50	1.51	66.3
69.7°N	121.4	lor_0035211483_0x630_sci_1	07:06:02.886	9.31	2.25	99.1
52.3°N	98.0	lor_0035211483_0x630_sci_1	07:06:02.886	3.06	2.00	88.3
52.2°N	98.6	lor_0035211488_0x630_sci_1	07:06:07.886	0.34	1.97	86.8
52.0°N	98.5	lor_0035211488_0x630_sci_1	07:06:07.886	1.10	1.79	78.8
51.9°N	98.1	lor_0035211488_0x630_sci_1	07:06:07.886	1.93	1.87	82.6
51.3°N	188.8	lor_0035219288_0x630_sci_1	09:16:07.886	2.23	2.19	99.1
60.2°S	116.7	lor_0035211843_0x630_sci_1	07:12:03.000	0.99*	1.55	68.3
66.0°S	190.0	lor_0035219643_0x630_sci_1	09:22:02.886	15.66	2.76	125.0
68.4°S	118.8	lor_0035211848_0x630_sci_1	07:12:07.885	0.64	2.23	100.8
68.9°S	222.6	lor_0035219648_0x630_sci_1	09:22:07.886	0.93	2.34	105.7
71.2°S	203.1	lor_0035219463_0x630_sci_1	09:19:02.885	0.60	1.77	79.9
73.7°S	207.1	lor_0035219648_0x630_sci_1	09:22:07.886	1.28	2.34	105.7

*Sum of double flash.

References and Notes

1. B. A. Smith *et al., Science* **204**, 951 (1979).
2. A. F. Cook, T. C. Duxbury, G. E. Hunt, *Nature* **280**, 794 (1979).
3. W. J. Borucki, A. Bar-Nun, F. L. Scarf, A. F. Cook II, G. E. Hunt, *Icarus* **52**, 492 (1982).
4. J. A. Magalhães, W. J. Borucki, *Nature* **349**, 311 (1991).
5. W. J. Borucki, J. A. Magalhães, *Icarus* **96**, 1 (1992).
6. B. Little *et al.*, *Icarus* **142**, 306 (1999).
7. U. A. Dyudina *et al., Icarus* **172**, 24 (2004).
8. U. A. Dyudina *et al.*, *Icarus* **160**, 336 (2002).
9. J. W. Warwick *et al.*, *Science* **212**, 239 (1981).
10. J. W. Warwick *et al.*, *Science* **215**, 582 (1982).
11. D. A. Gurnett *et al.*, *Science* **307**, 1255 (2005).
12. G. Fischer *et al. Icarus* **190**, 528 (2007).
13. U. A. Dyudina *et al. Icarus* **190**, 545 (2007).
14. A. F. Cheng *et al.*, *Space Sci. Rev.*, in press (available at http://arvix.org/abs/0709.4278v1).
15. Nighttime polar images were obtained with LORRI from 5.6×10^6 to 5.8×10^6 km over a 2.3-hour period on 3 March 2007 with 5.0-s exposure times. Pixel resolution is 28 km/pixel on the sky, corresponding to 50 km in latitude at 60°N.
16. Lightning strikes could be distinguished from cosmic ray hits and auroral features by their distinctive shapes. Because of slight spacecraft nodding motions, constant-brightness point sources such as stars produce curlicue features in our 5-s exposures, unlike our short-lived lightning strikes. Lightning flashes produce a bright central flash surrounded by a halo of light due to diffuse scattering by the overlying atmosphere. Lightning energies were calculated using the spectral irradiance of jovian lightning determined by Borucki *et al.* (*31*). The latitudes and longitudes of lightning flashes are determined by a limb/terminator fitting program that generates the planetary ellipse based on the range, camera focal length, and pixel scale. With sufficient contrast between the sky and the planet, the ellipse center is located with an iterative least-squares fit, typically with a precision of 0.1 pixel or better. For low-contrast images, the ellipse is placed manually with an uncertainty of a few pixels.

17. W. J. Borucki, M. A. Williams, *J. Geophys. Res.* **91**, 9893 (1986).
18. S. J. Weidenschilling, J. S. Lewis, *Icarus* **20**, 465 (1973).
19. C. P. Porco *et al.*, *Science* **299**, 1541 (2003).
20. A. P. Ingersoll *et al.*, *J. Geophys. Res.* **86**, 8733 (1981).
21. S. S. Limaye, *Icarus* **65**, 335 (1986).
22. M. Allison, *Icarus* **83**, 282 (1990).
23. K. H. Baines, R. W. Carlson, L. W. Kamp, *Icarus* **159**, 74 (2002).
24. P. J. Gierasch *et al.*, *Nature* **403**, 628 (2000).
25. A. P. Ingersoll, C. C. Porco, *Icarus* **35**, 27 (1978).
26. I. A. Pirraglia, *Icarus* **59**, 169 (1984).
27. D. C. Reuter *et al., Space Sci. Rev.*, in press (available at http://arxiv.org/abs/0709.4281v1).
28. Galileo NIMS global maps were acquired on 5 September 1996 from a distance of 1.98×10^6 km, a phase angle of 64.3°, a subsolar latitude near 2°S, and a subspacecraft latitude near 0°. A Cassini Imaging Science Subsystem global image was acquired on 29 December 2000 from a distance of approximately 1.0×10^6 km, a phase angle near 90°, a subsolar latitude near 2.9°N, and a subspacecraft latitude near 3.5°N. A New Horizons LEISA global map was acquired on 28 February 2007 in three north/south scans over a 47-min period beginning at 01:40 universal time (UT) on 28 February from an altitude of 2.32×10^6 km, a phase angle of 76°, a subsolar latitude near 2.9°S, and a subspacecraft latitude of 8.4°S. The three-color image (middle right of Fig. 2), is composed of a 1.59-μm continuum wavelength image (red), a 1.90-μm wavelength image of moderate atmospheric gas absorption (green), and a 1.85-μm wavelength image of relatively strong absorption gas (blue). Blue accentuates high-altitude clouds and hazes above the 300 mbar level, green depicts clouds most prominently near and above the 600-mbar level, and red shows clouds down to several bars. The 4.8-μm pseudo-color images were acquired at NASA's Infrared Telescope Facility (IRTF) at 10:08 UT on 30 December 2000 by the National Science Foundation camera (NSFCam) camera and on 18 March 2007 at 14:53 UT by the NSFCam2 camera. The 17.9-μm images were acquired by the Jet Propulsion Laboratory's MIRLIN (Mid-Infrared Large-well Imager) camera (*32*) at 5:50 UT on 29 December 2000 and by the MIRSI (Mid-Infrared Spectrometer and Imager) camera/spectrometer (*33*) at 16:12 UT on 18 March 2007.
29. A. R. Vasavada *et al., Icarus* **135**, 265 (1998).
30. D. C. Reuter *et al., Science* **318**, 223 (2007).
31. W. J. Borucki, C. P. McKay, D. Jebens, H. S. Lakkaraju, C. T. Vanajakshi, *Icarus* **123**, 336 (1996).
32. M. E. Ressler *et al., Exp. Astron.* **3**, 277 (1994).
33. L. Deutsch, *et al., SPIE* **4841**, 106 (2002).
34. We thank the New Horizons mission and science teams. New Horizons is funded by NASA. G.S.O., P.Y.F., and B.M.F. were visiting astronomers at the IRTF, which is operated by the University of Hawaii under Cooperative Agreement no. NCC-538 with NASA, Science Mission Directorate, Planetary Astronomy Program. Thanks to E. Tollestrup and M. Connelley for IRTF instrument orientation and J. Kemerer' and J. Yang for assistance in reducing the observations. Much of the work described in this paper was carried out at the Jet Propulsion Laboratory, Pasadena, CA, under contract with NASA.

17 July 2007; accepted 19 September 2007
10.1126/science.1147912

REPORT

Jupiter's Nightside Airglow and Aurora

G. Randall Gladstone,[1]* S. Alan Stern,[2] David C. Slater,[1] Maarten Versteeg,[1] Michael W. Davis,[1] Kurt D. Retherford,[1] Leslie A. Young,[3] Andrew J. Steffl,[3] Henry Throop,[3] Joel Wm. Parker,[3] Harold A. Weaver,[4] Andrew F. Cheng,[2] Glenn S. Orton,[5] John T. Clarke,[6] Jonathan D. Nichols[6]

Observations of Jupiter's nightside airglow (nightglow) and aurora obtained during the flyby of the New Horizons spacecraft show an unexpected lack of ultraviolet nightglow emissions, in contrast to the case during the Voyager flybys in 1979. The flux and average energy of precipitating electrons generally decrease with increasing local time across the nightside, consistent with a possible source region along the dusk flank of Jupiter's magnetosphere. Visible emissions associated with the interaction of Jupiter and its satellite Io extend to a surprisingly high altitude, indicating localized low-energy electron precipitation. These results indicate that the interaction between Jupiter's upper atmosphere and near-space environment is variable and poorly understood; extensive observations of the day side are no guide to what goes on at night.

Jovian dayside airglow and aurora have been extensively observed from Earth orbit since their initial detection during the Voyager flybys in 1979 (*1*–*8*). On 3 March 2007 between 06:28 and 09:58 universal time (UT) (about 3 days after closest approach on 28 February at 05:43 UT) during the flyby of Jupiter, the New Horizons spacecraft made several high phase-angle observations of nightside airglow (nightglow) and auroral emissions. Because the night side has not been well observed, longstanding questions remain, including the nature of Jupiter's 121.6-nm (Lyα) nightglow (for example, is it similar to the tropical arcs of Earth?), how the nightside auroras are different from those on the day side, and what the smallest structures in satellite footprint auroras are and what governs their size.

[1]Southwest Research Institute, San Antonio, TX 78238, USA. [2]NASA Headquarters, Washington, DC 20546, USA. [3]Southwest Research Institute, Boulder, CO 80302, USA. [4]The Johns Hopkins University Applied Physics Laboratory, Laurel, MD 20723, USA. [5]Jet Propulsion Laboratory, Pasadena, CA 91109, USA. [6]Boston University, Boston, MA 02215, USA.

*To whom correspondence should be addressed. E-mail: rgladstone@swri.edu

Jupiter's nightside hydrogen Lyα airglow was seen by Voyager 2 in 1979. Data from its ultraviolet (UV) spectrometer showed substantial nonauroral emissions well past the terminator, which were interpreted to result from low-latitude particle precipitation (*1*, *2*). Low-latitude particle precipitation was also suggested as a way to maintain Jupiter's large exospheric temperature (*9*) and to account for low-latitude x-ray emission (*10*). In contrast, several nightside east-west scans by the Alice UV spectrograph on New Horizons (*11*, *12*) indicate that the Lyα nightglow is faint, and there was no evidence of emission from high solar zenith angle regions on the night side that are far from the auroral regions (Fig. 1). Instead, the emissions are well fit by scattered solar Lyα radiation from the bright limb (*13*). This finding implies that no substantial low-latitude particle precipitation is currently occurring and suggests that either the Voyager results were spurious or Jupiter has changed between the two epochs (the Voyager flybys were during solar maximum, whereas the New Horizons flyby occurred during solar minimum).

Observations of Jupiter's night side also provide a way to search for the presence of tropical arcs, which at Earth are bands of emission on either side of the magnetic equator resulting from the recombination of ions and are useful tracers of ionospheric dynamics (*14*, *15*). The Lyα dayglow of Jupiter is known from Voyager Ultraviolet Spectrometer results to have a bulge of brightness that follows the magnetic dip equator (*16*). A possible explanation for the Lyα bulge is extra scattering of solar Lyα radiation from a hot hydrogen population resulting from H_3^+ recombination on either side of the magnetic equator; that is, the bulge might resolve into tropical arcs if seen at higher spatial resolution (*17*). Although no large-scale Lyα nightglow was seen by New Horizons, there are indications of excess brightening near the terminator, especially in regions where tropical arcs might be expected (such as near the end points of the low-latitude magnetic field line traces in Fig. 1).

Most of Jupiter's UV aurora results from collisions of energetic magnetospheric electrons with atmospheric hydrogen, leading to emissions at wavelengths from 80 to 165 nm. However, the more energetic electrons penetrate deeper into the atmosphere, where the resulting shorter-wavelength UV auroral emissions can be partially absorbed by atmospheric methane. The color ratio is defined as the ratio of the integrated auroral brightness from 155.7 to 161.9 nm over that from 123.0 to 130.0 nm (*18*, *19*) and is used as a proxy for the mean energy of auroral electrons. A larger color ratio results from preferential absorption of shorter-wavelength UV photons by hydrocarbons (primarily CH_4) overlying a deeper layer of auroral emissions. Data from the Space Telescope Imaging Spectrograph (STIS) on the Hubble Space Telescope (HST) (*20*) and the Ultraviolet Imaging Spectrograph on Cassini (*21*) show that typical color ratios were 1.5 to 6.0 and that the largest ratios (and presumably